Next generation optoelectronic components enabled by direct write microprinting technology

Donald J. Hayes and Ting Chen
*MicroFab Technologies, Inc.

ABSTRACT

Direct write microprinting technologies are now being developed and used across a wide spectrum of optoelectronic applications, because they provide opportunities for manufacturing a series of components in micrometer scales and in large array size with reduced cost. Micro-optic structures have been printed not only as stand-alone components, but also directly onto other active and passive components, such as VCSEL, photodiode, optical fiber, etc., to form high performance assemblies. These assemblies can be further integrated with electronic circuits via solder ball printing to construct miniature and high sensitivity sensing devices, such as photodiode array detector, fluorescence probe, etc. By implementing MEMS technologies, micro-clampers have also been developed for the alignment and packaging of miniature, multi-channel sensing devices.

Keywords: microprinting, inkjet printing, micro-optics, microlens, SolderJet®, fluorescence probe, lensed fiber

1. INDRODUCTION

Interest in utilizing direct write microprinting for optoelectronic manufacturing has increased in recent years due to the advantages it provides in high-level automation, material and labor cost reduction, and environmental friendliness. The printing process is noncontact, data driven, and no masks or screens are required. This technology can be flexibly applied to a broad range of materials and substrates to form a variety of structures – from micro-optic components to solder ball interconnects, and thus has extensive applications in sensing and detections. Due to the small scale and large array size of the printed structures, this technology also offers advantages in miniaturization and parallel processing of the sensing devices. After giving a brief background review of microprinting methods, we will present concepts and results of optoelectronic components fabricated by using this technology.

2. BACKGROUND OF INKJET PRINTING

In piezoelectric-based, drop-on-demand (DOD) microjet or inkjet printing systems the application of a voltage pulse to a piezoelectric transducer that is coupled to the fluid induces a volumetric change in the fluid within a printing device. The pressure/velocity transients occurred in the fluid are directed to produce droplets from the orifice of the device.[1] The process of droplet formation and ejection from the orifice of a DOD device is shown in the time-sequenced photos of Figure 1. The volumes of the printed materials at target locations are determined by the size (20-100μm) and number of dispensed droplets. The shape of deposited material is determined by the surface tensions of the material and the substrate surface at their boundary. Polymeric formulations remain liquid until solidified by UV irradiation, whereas solder alloy droplets printed at temperature slightly above their melting point freeze upon contact with the substrate. Printheads for dispensing these materials consist of a printing device attached to a fluid reservoir, both of which are typically heated to maintain the fluid at the DOD jetting threshold of ≤ 40 centipoise for polymer jetting, or slightly above the melting point for solder alloy printing.[2] The printing devices are of two configurations, single and multiple channels.

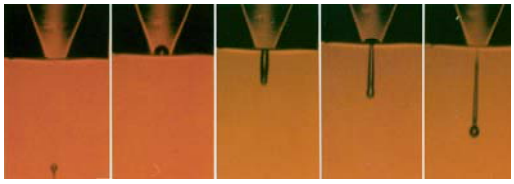

Figure 1. Sequence (left-to-right) of formation and ejection of a 50 μm diameter droplet from a drop-on-demand inkjet device.

* microinfo4@microfab.com; phone 1-972-578-8076; fax 1-972-423-2438; MicroFab Technologies, Inc., 1104 Summit Ave., Suite 110, Plano, TX 75074 USA; http://www.microfab.com.

The latter may consist of ganged single jets or monolithic array devices. The single-channel device, as shown in Figure 2, typically consists of a cylindrical piezoelectric element attached to a glass capillary tube with an orifice formed by heating. The array print head, as exemplified in Figure 3, may be fabricated by machining channels in a block of PZT, laminating a cover, and attaching an orifice plate. The single-jet devices can be operated at temperatures up to 300°C, for dispensing SnAu solder, although most of the development work to date has been with eutectic 63Sn/37Pb solder. Droplets may be dispensed at frequencies up to 10,000 drops/sec, utilizing either step-and-print or print-on-fly modes.

Figure 2. Single-jet device for micro-dispensing up to temperatures of 300°C.

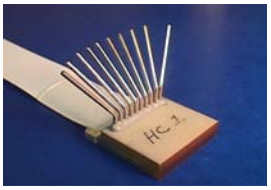

Figure 3. Array printing device, 1 inch wide, for micro-dispensing up to 10 different fluids.

A new inkjet printing platform that can utilize any of these device configurations and dispense polymeric, solder or biomedical materials is shown in the photograph of Figure 4. It consists of two basic structures, the printing chamber and the control console. The layout of key elements within the printing chamber is illustrated in Figure 5. The motion system consists of precision X, Y & θ stages for supporting and moving the substrate chuck, along with a Z stage for supporting and moving the overhead assembly that includes a bank of four print heads with individual temperature and pneumatic controls, a camera for viewing printed material and substrate fiducials, and an on-stage UV curing head with N_2 gas co-flow. The printing data are created directly from CAD information and the printing process is controlled by the software. This platform provides great accuracy and flexibility for printing a variety of micro-arrays and macro-structures with different materials.

Figure 4. JetLab® printing station for direct writing from data files of patterns and consisting of 4 printheads, XYZ & θ stages, UV-curing head, N_2 co-flow, pneumatic & temperature controls, and software.

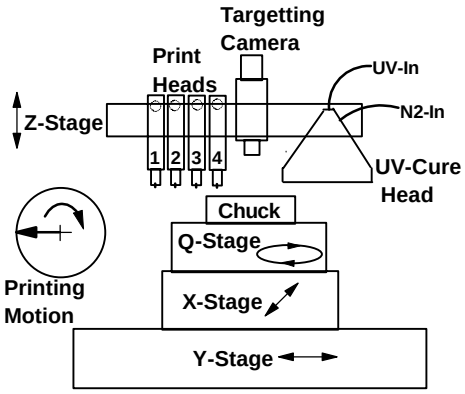

Figure 5. Schematics of layout of key elements of printing station and of simultaneous use of rotary and linear motions.

3. MICRO-OPTICS FOR DETECTION DEVICES

In many sensing applications, the excitation or illumination light, such as output from LED, diode laser, VCSEL, or optical fiber, has specific diverging angle or numerical aperture (NA). On the other hand, the receiving or detecting element, such as photodiode or optical fiber, has a limited active areas and receiving NA. A mismatch at each light coupling interface will waste light energy and reduce the detection sensitivity. In array configurations, improper beam shapes can cause cross-talks among different channels. Microlenses have been widely used in beam shaping for optoelectronic applications. The fabrication of microlens array and lensed fiber array by microprinting has the advantages of flexibility, low cost, and easy integration with other components.

3.1 Microlens materials

The preferred class of materials for microlens printing is UV-curing optical epoxies.[2] The 100%-solid formulation consists of liquid state monomers, which solidify upon UV radiation. The material is optically transparent from visible to

near infrared. Anti-reflective (AR) coatings can be applied to reduce the reflection loss. This class of materials has superior thermal and chemical durability, compared to other optical-grade plastics such as acrylics, photoresists, and thermoplastics. For example, no changes in focal lengths of such lenses, within our measurement resolution of 2-3%, were seen at elevated temperatures up to 100°C. Additionally, no significant change in focal length at room temperature has been seen for optical epoxy microlenses after either exposure to thermal aging for thousands of hours at 85°C or to one-hour thermal cycles at temperature as high as 200°C. The microlenses also have high mechanical strength and can sustain harsh environments of the successive processes, such as dicing, bonding, etc.

3.2 Microlens arrays

Arrays of microlenses, such as that shown in Figure 6, are currently printed in the range from 20 μm to a few mm in diameter.[3] We have shipped microlens arrays for the use in coupling of light in/out optical fibers, light collection to silicon detectors, LED array module, VCSEL array module, etc. With precision fabrication processes, lens diameter and location can be controlled to within ± 1μm. With a fixed diameter, the change in volume will translate to the change in the lens height (sag) or in the radius of curvature of the spherical surface. This process of building microlens aspect ratio digitally is accomplished by computer programming integrated into the control software of the printing platform. The minimum height (hence, the longest focal length) is limited by the smallest volume of material, which can be made to flow sufficiently to achieve the diameter; while the maximum height (hence, the shortest focal length) is limited by the surface tensions of lens material and substrate at the liquid-solid boundary. The resolution of lens height and focal length is limited by the drop size. Since the drop number is adjusted in integers, the higher the number of drops printed to achieve the requisite lens volume, the higher the resolution will be. With this capability microlens in the range of f/1 to f/5 have been fabricated. Figure 7 is an example of 700 μm microlenses printed with different numbers of 43 μm diameter drops.

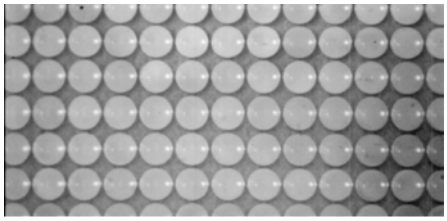

Figure 6. Printed array of 916 μm diameter microlenses on 1 mm centers with focal lengths of 1.10 ± 0.01 mm.

Figure 7. 700 μm diameter microlenses in profile with focal lengths of (left-to-right) of 850, 525, 430 and 405 μm, respectively.

3.3 Lensed fibers

Inkjet technology can be utilized to print a small spherical microlens onto the center of the tip of a single/multi mode optical fiber, as shown in Figure 8, to form a monolithic device for increasing the efficiency of light coupling or the collection between fiber and other optical/optoelectronical components. Another assembly configuration is show in Figure 9, where the fiber tip is inserted with an offset distance into a glass collet. The inside diameter (I.D.) of the collet matches the outside diameter (O.D.) of the fiber. The optical epoxy is printed to fill up the funnel of the collet and to form a hemispherical microlens, as shown in Figure 10. The structural parameters of this assembly - offset distance, collet O.D., and lens height - are decided by the fiber type, the refractive index of optical epoxy, and the optical performance specifications (collimation or focusing). The performance of a lensed single mode fiber is presented as the curves of beam width (at 13.5% intensity level) vs. axial distance in Figure 11. The single mode fiber, working at 633 nm, has core/clad diameter of 4.3/125 μm. The collet O.D is 1.78 mm and the offset distance is 2.48 mm. The 3 curves are with respect to the lens heights of 0.553, 0.563, and 0.582 mm. The divergence of the bare fiber with NA=0.11 is

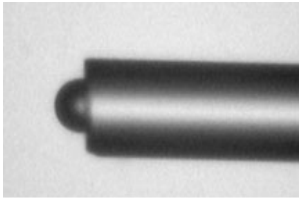

Figure 8. A 70 μm diameter microlens printed onto the tip of a 125 μm diameter optical fiber to increase NA.

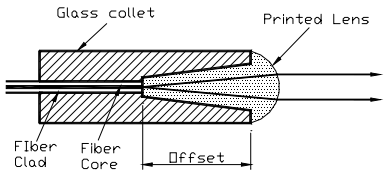

Figure 9. Concept of lensed fiber fabricated by inkjet printing.

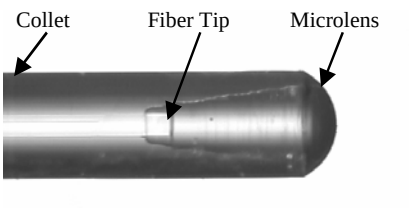

Figure 10. Fabricated lensed fiber.

also given for comparison. Lensed fibers have also been assembled for other types of fibers: multi-mode, sensor grade and power delivery fibers. Figure 12 gives an example of lensed sensor-grade fiber. The fiber has core/clad diameter of 200/230 μm. Its NA is 0.18 at 50% intensity level. The collet O.D. is 1.53 mm and the offset distance is 2.50 mm. Figure 12 shows that the focus spot size is 0.35 mm at a distance of 3.5 mm from the lens vertex for lens height 0.433 mm; while the focus spot size is 0.60 mm at a distance of 5.5 mm for lens height 0.361 mm.

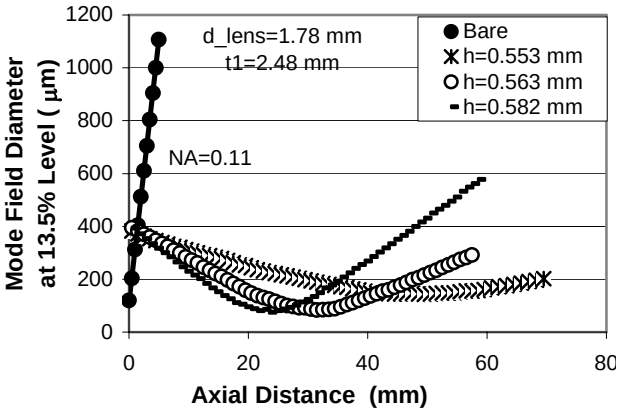

Figure 11. Beam width vs. axial distance of lensed single mode fiber.

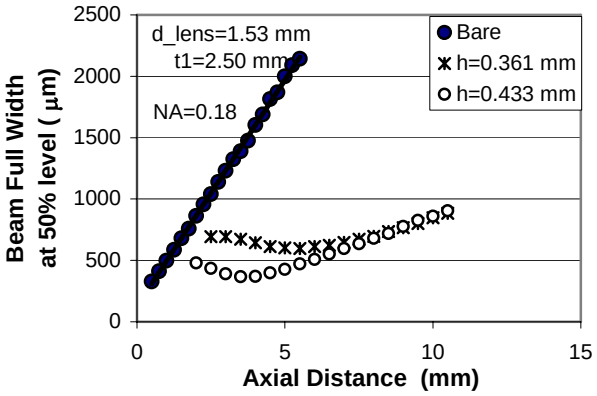

Figure 12. Beam width vs. axial distance of lensed sensor-grade fiber.

4. MICRO-OPTICS FOR BIOCHEMICAL SENSING

Biochemical fiber optic sensors in use today typically consist of an indicator attached to a single fiber, where the indicator chemistry is designed to change its optical properties (e.g., fluorescence or absorption) quantitatively in response to a target chemical composition and property, such as oxygen content, pH value, and electrolyte (K+, Ca++, Li+, etc.), under illumination of a suitable wavelength.[4] The absorption or re-emission of the illuminating radiation in the form of fluorescence is monitored via photosensitive detectors with a separate sensor required for each target agent. Multi-functional fiber optic bio-chemical sensors have potential use in clinical diagnosis, manufacturing process control, weapon detection, environmental monitoring, etc. Multifunctional array sensors have been fabricated previously with fiber imaging bundles using a series of steps to "grow" sequentially indicator elements by masking the end of the fiber and UV curing each element out of different polymeric solutions, but poor uniformity and reproducibility of indicator element geometries have required calibration of each fiber and have limited their use.

Microprinting technology allows a reproducible fabrication of multifunctional fiber-optic sensors on the same optical fiber bundle. UV-curing optical epoxies are adjusted to provide enhanced porosity over the formulations used for microlens printing and doped with biochemical indicators. They may be printed into patterns of sensor elements onto the tips of imaging fiber bundles, providing a sensor configuration. Figure 13 shows an array of 80 μm diameter hemispherical indicator elements printed onto a 480 μm diameter optic fiber bundle, fluorescing under UV illumination. The unique opportunity provided by inkjet printing technology in the area is the low cost, high throughput, and reproducible fabrication of a large number of uniformly sized sensor elements consisting of different indicator chemistries on the same optical fiber bundle, in order to provide multi-functionality in a monolithic sensor. Signals from different indicator elements are distinguished by spatial and spectral filtering in the detector system. Initial characterization of fluorescing intensities from the seven elements has shown an element-to-element variation of less than 5%.

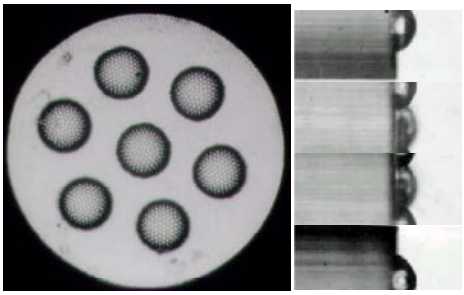

Figure 13. Array of 80 μm diameter hemi-spherical indicator elements printed onto 480 μm diameter fiber bundle, shown from above (left) and in profile (right). (Fiber bundle courtesy of B. Coleston and S. Brown of Lawrence Livermore National Laboratories.)

5. MINIATURE AND ARRAY SENSING AND PROCESSING DEVICES

Micro-optic structures have been printed in large array configurations for data interconnect and process. They can also be printed directly to other active components, such as vertical cavity surface emitting lasers (VCSELs) and photodiodes (PDs), to form high performance assemblies, which can be further integrated with electronic circuits via solder ball printing to fabricate miniature and high sensitivity detection devices, such as photodiode array detector, fluorescence probe, etc. By implementing MEMS technologies for self positioning and alignment, more complex devices can be fabricated with low cost.

5.1 Microlens in the smart-pixel array

VCSELs have been well recognized as low cost light sources. They can be fabricated monolithically in a very large scale. Because the light beam is emitted perpendicular to the surface, VCSELs are tested at wafer level. One-dimensional and two-dimensional arrays can be diced from a wafer directly. PDs are fundamental light detection devices. With the integration of Si ASICs, a smart pixel array can perform optical detection and inter-connect with computational enhancement by VLSI architectures.[5] Figure 14 (top) shows a smart pixel, consisting of a VCSEL array and an adjacent detector array with two microlenses above for collimating the laser output beam and focusing a return beam into the detector elements. Printed microlenses were selected for this application based on their greater coupling efficiency and the wavelength independence of a refractive lens compared to diffractive ones. Photographs of this smart pixel module and the printed microlens array incorporated in it are shown in Figure 14 (bottom). These arrays are printed in 32 chip patterns onto 3-inch diameter, thin quartz wafers. Each chip consists of two each 16 x 16 identical arrays of 250 μm diameter, 60 μm sag microlenses, giving a total of 16,384 microlenses per wafer. The microlenses in each array are printed on 500 μm centers, and the two arrays are offset from each other by 250 μm along a diagonal.

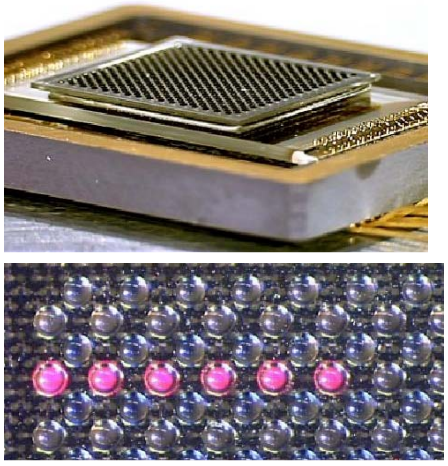

Figure 14. Smart pixel array module (top) and printed 250 μm diameter microlens array in module with VCSELs under 6 lenslets turned on (bottom). (Photo courtesy of Y. Liu & A. Cox of Honeywell)

5.2 Lensed VCSEL array and photodiode array fabricated on wafer level

VCSELs and PDs are often paired for applications in fiber optic interconnects. They have also found numerous applications in detection sensors, position sensors, scanners, etc. Almost all application of these photonic devices require the presence of micro-optics to collimate or converge the emitting or receiving light beam to increase optical coupling efficiency. For this purpose, ball lenses and V-grooves have been used for the beam shaping. However, these structures are difficult to implement, when the element spacing becomes as small as 250 μm. Microlens arrays, along with a spacer, have been used for the VCSEL light collimation. However, this structure has a very stringent tolerance in alignment accuracy. Inkjet printing can provide a solution for a wafer level integration of VCSEL/PD and micro-optics with significant cost reduction. The integration concept is given in Figure 15 and 16. A transparent pedestal is fabricated directly on VCSEL or PD, and the optical epoxy is printed on top of the pedestal to form a microlens. The resulting beam shaping is decided by the selection of the dimensions of micro-optic structures (pedestal and microlens) and the

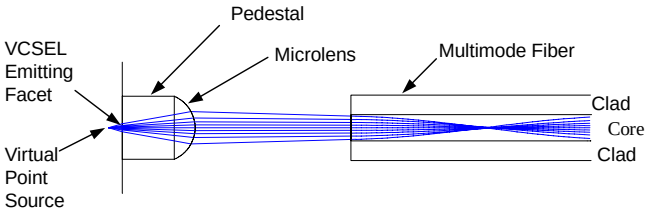

Figure 15. Integration of pedestal and microlens with VCSEL for light coupling to multimode fiber.

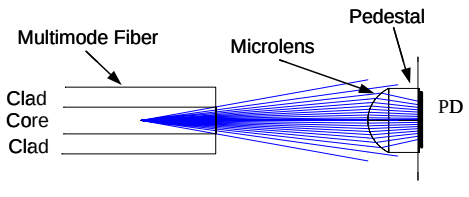

Figure 16. Integration of pedestal and microlens with PD for light coupling from multimode fiber to PD.

indices of refraction of the materials. For an effective coupling from VCSEL to graded-index multimode fiber (MMF), pedestals are typically 100 – 120 μm in diameter and 70 – 120 μm in height, and the microlenses are typically 30 - 40 μm in height. The coupling from MMF to PD is less critical, due to the relatively large active area of PD. In this case the pedestals are typically 100 – 120 in diameter and 40 – 80 in height, and the microlenses are typically 30 – 40 μm in height. The micro-optics enhance the light collection and, therefore, enhances the detection sensitivity. The pedestals are fabricated in a photolithographic process of very-thick film patterning, and, therefore, has high alignment accuracy with the VCSELs or PDs. The alignment from microlens to pedestal has a self-alignment nature.

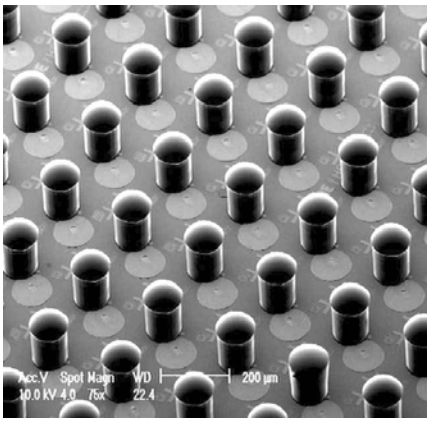

Figure 17. Wafer level fabrication of pedestals and microlenses on VCSEL wafer.

Figure 17 shows a pedestal-microlens array on a VCSEL wafer. The pedestals have uniform, clean finishing with vertical side walls. The bond pads, which appear as circular features on the wafer surface, are well exposed after the process. The processed wafers were then diced into arrays. For evaluation, the microlenses were printed with different lens heights. Figure 18 shows the coupling efficiency from VCSEL to MMF, measured at varying axial distance from the VCSEL's emitting facet to the fiber entrance surface. The drop number for microlenses varies from 3 to 7, corresponding to lens height change from 25 to 38 μm. Data of butt coupling are also presented for comparison. An AR coating can be applied for further reduction of coupling loss. The DC characteristics of the VCSELs were not changed by the construction of the micro-optics, as shown in Figure 19. The monolithic lensed VCSEL array not only has improved optical coupling efficiency, but also can be easily assembled into higher level components.

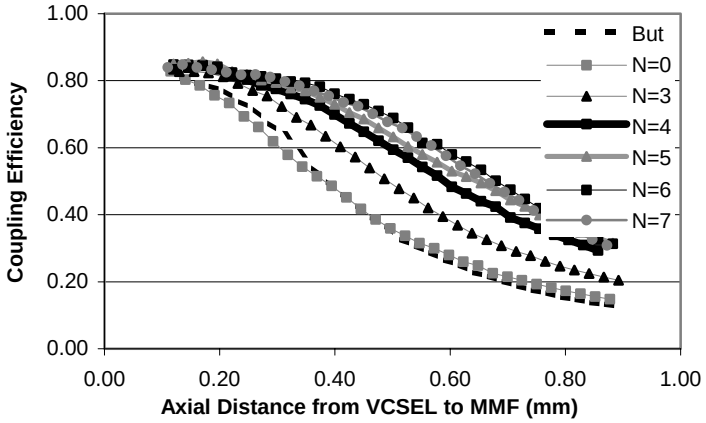

Figure 18. Coupling efficiency from VCSEL to MMF for different epoxy drop number N printed on pedestals.

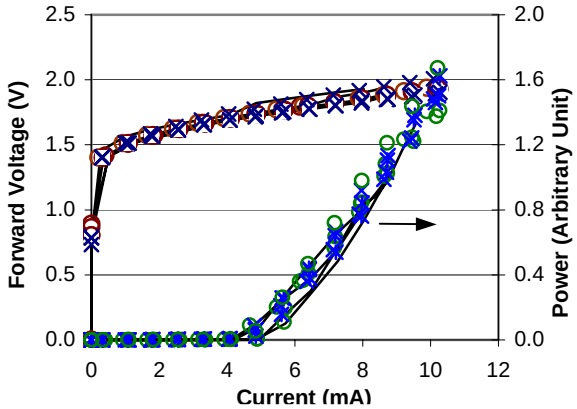

Figure 19. DC characteristics of VCSELs: dashed lines – baseline VCSELs; open circles – VCSELs with pedestals; cross marks – VCSELs with pedestals and microlenses.

5.3 Electrical interconnects of direct solder bonding by SolderJet®

Microprinting of molten solder can be used for electrical interconnects in miniature sensing and detection structures,[6] in which many times wire bonding is not feasible. Figure 20 exemplifies the solder bonding of a 1 x 4 VCSEL die to a PCB test coupon. Figure 21 exemplifies the solder bonding of a 1 x 4 PD die to a PCB test coupon. The solder balls connect the anode bond pads on the die with the metal leads on the coupon, and one or more solder balls connect the cathode metallization on the back side of the die with the lead on the coupon. Solder printing is not only accurate in position targeting and in dispensed volume, but also has minimal thermal impact to the

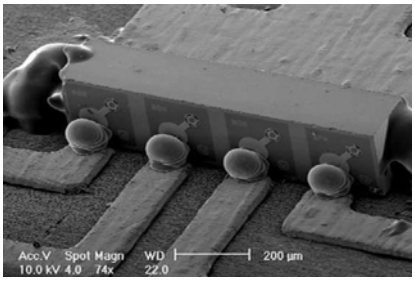

Figure 20. Direct VCSEL die bonding using SolderJet® .

work piece. VCSEL's DC emission characteristics were not changed by the SolderJet® bonding, as shown in Figure 22; same is true for the PD's DC responsivity, as shown in Figure 23.

With a combination of the SolderJet® bonding and the micro-optics, miniature VCSEL array module and PD array optical subassembly can be fabricated for array illumination and detection. They can be further integrated with driver and receiver ICs to form compact modules. The PD array sensor module can be used for rapid weak-fluorescence detection with parallel digital readout.

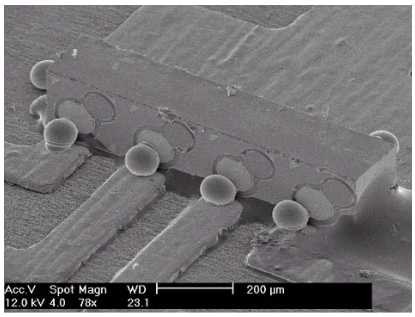

Figure 21. Direct PD die bonding using SolderJet®.

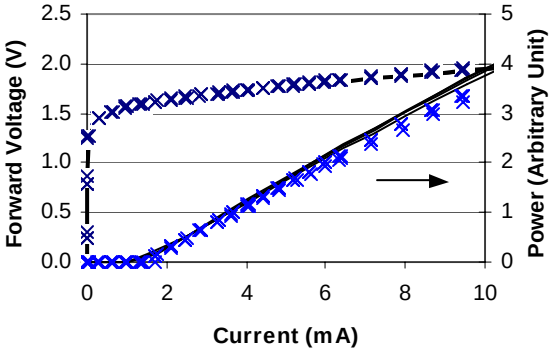

Figure 22. DC characteristics of VCSELs: solid curves – before solder bonding; cross marks – after solder bonding.

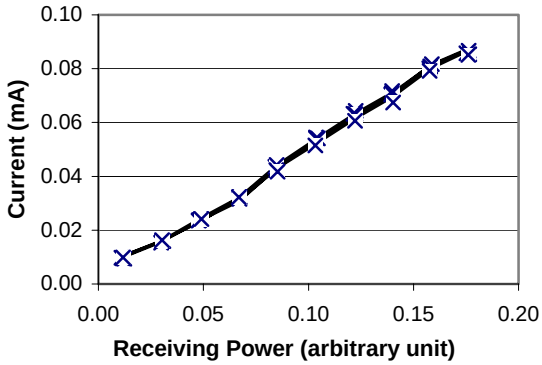

Figure 23. DC Responsivity of PDs: solid curves – before solder bonding; cross marks – after solder bonding.

5.4 MEMS technology for alignment and packaging of miniature sensing device

In miniature sensing devices the alignment of active and passive optoelectronic components is important to the system efficiency. The alignment can be very critical in the case of weak signal detection. Normally, the optical alignment accuracy needs to be controlled to within a few micron. The system design has also to deal with issues like electrical interconnect, thermal dissipation, packaging, etc. We have developed a micro-electro mechanical systems (MEMS) based metallic clamper for the optical/electrical self-alignment and interconnect. The MEMS clamper has a two-layered structure. The bottom layer, which is 20 µm thick electroplated copper, is patterned for electrical routing and bonding. The top layer, which is partly suspended 100 µm thick electroplated nickel, comprises of the actual MEMS clamper. Several versions of clampers have been designed and fabricated, one of which is shown in Figure 24. The arms of the clamper can be stretched out to have a die placed between them. Once the arms are released, they clamp in the die to the desired position with ± 2 µm accuracy, as seen in Figure 25, in which a lensed VCSEL die is clamped in position. Same clampers in an array or different clampers in specific locations can be fabricated on a common substrate to hold different active or passive parts - dies, ferrules, microlens, micro-mirror, etc. Because the alignment of these parts is ensured by the MEMS design and the photolithographic process, the assembly procedure can be greatly simplified. In comparison with other mechanical–only micro-positioning structures, such as silicon grooves, this design also provides electric interconnections. This can, in many cases, ease the packaging difficulties of miniature devices.

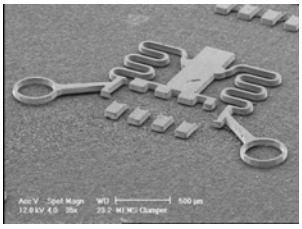

Figure 24. MEMS based metallic clampers for mechanical positioning and metal pads for electrical connections.

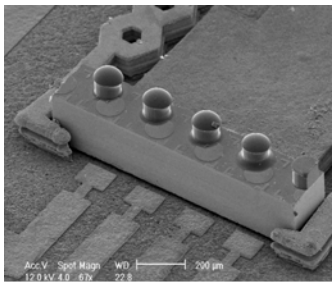

Figure 25. A lensed VCSEL die is positioned by a MEMS clamper.

5.5 Fluorescence probe

The lensed fibers with specific characteristics, as described in Section 5.2, can be assembled to construct a fiber fluorescence probe for a localized, weak signal detection. The conceptual schematic is illustrated in Figure 26. The light from a white light source passes through a short-pass filter and then is launched into a UV-VIS grade fiber by a coupler unit, which consists of a macrolens and a microlens assembled to the fiber tip (LF1). The output light from this fiber is focused and directed to a small spot by the microlens assembled at the tip of the fiber LF2. The fluorescence emission is coupled to read fibers bundled in the same probe head. The read fibers also have microlenses at their tips (LF3 and LF4) to increase fluorescence collection. The read fibers are separated from the bundle at a trifurcation place. Their outputs are coupled to detectors through microlenses (LF5 and LF6). Facilitated with different band pass filters before the detectors, the probe can detect simultaneously fluorescence in different spectrum ranges. The probe head can be mounted to a controlled motion system for scanning through an area with accurate spatial addressing. This probe will have the advantages of high sensitivity and high throughput.

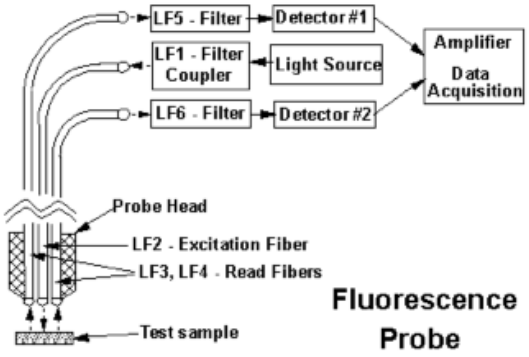

Figure 26. Schematics of a fluorescence probe and detection system.

6. CONCLUSIONS

We have shown that the microprinting of optical epoxy can be employed to fabricate stand-alone micro-optic components, such as precision microlens arrays and lensed fibers. The microoptic structures can also be printed directly onto active/passive optoelectronic devices - VCSELs, PDs, and fiber bundle - to form high performance assemblies for sensing and detection applications with parallel data processing capabilities. The microprinting of solder balls can be employed for direct die bonding in miniature detection devices. In addition, a MEMS based metallic clamper and associated electrical lead pattern can be fabricated for the positioning of dies/ferrules and electrical connections. All the high precision fabrication methods presented here have the nature of self-alignment that simplifies device assembly and, therefore, reduces the fabrication cost.

ACKNOWLEDGMENTS

This work has been supported in part by the U.S. Air Force Research Labs, by DARPA via the U.S. Army Research Office and U.S. Army Aviation and Missile Defense Command, and by the National Science Foundation. The authors acknowledge the technical development work of MEMS clampers by A-.K.C. Nallani and J-.B. Lee of University of Texas at Dallas.

REFERENCES

1. D.B. Wallace, W.R. Cox, and D.J. Hayes, “Direct write using ink-jet techniques”, Eds. Alberto Pique and Douglas B. Chrisey, *Direct-write technologies for rapid prototyping applications – Sensors, Electronics, and Integrated Power Sources*, pp 177-227, Academic Press, San Diego 2002.
2. D. J. Hayes, W. R. Cox, and M. E. Grove, “Micro-jet printing of polymers and solder for electronics manufacturing”, *Jour. Electronics Manufacturing, 8*, pp 209-216, 1998.
3. T. Chen, W.R. Cox, D. Lenhard, and D.J. Hayes, “Microjet printing of high precision microlens array for packaging of fiber-optic components”, *SPIE Proceedings, 4652*, pp 136-141, 2002.
4. B.W. Coleston Jr., D.M. Gutierrez, M.J. Everett, S.B. Brown, K.C. Langry, W.R. Cox, P.W. Johnson, and J.N. Roe, “Intraoral fiber-optic-based diagnostics for periodontal disease”, *SPIE Proceedings, 3911*, pp 2-9, 2000.
5. Y. Liu, “Heterogeneous integration of OE arrays with Si electronics and microoptics”, *IEEE Transactions on Advanced Packaging, 25*, pp 43-49, 2002.
6. T. Chen, D.J. Hayes, D.B. Wallace, A-.K. C. Nallani, and J-.B. Lee, “Inkjet printing for optical/electrical interfacing of VCSELand PD arrays”, *IMAP International Symposium on Microelectronics Proceedings*, pp 864-868, 2003.